catalysts

MDPI

Supplementary Information for:

Influence of the $La_{0.2}Sr_{0.7}Ti_{0.95}Ni_{0.05}O_3$ (LSTN) Synthesis Method on SOFC Anode Performance

Supplementary Tables

Table S1. Rietveld refined lattice parameters, lattice strain and phase content of LSTN samples before and after exsolution, refined to cubic Pm-3m structure (PDF card no. 00-005-0634) and tetragonal I4/mcm (PDF card no. 04-025-4518).

		Cubic Pm-3m			Tetragonal I4/mcm			
		a_0 (A)	e_0	wt%	a_0 (A)	c_0 (A)	e_0	wt%
SS	Before exsolution	3.905	0.0006	87.1	5.511	7.847	0.018	12.9
	After exsolution	3.904	0.0005	92.5	5.72	8.832	0.018	7.5
SG	Before exsolution	3.904	0.0013	96.3	5.751	8.026	0.013	3.7
	After exsolution	3.904	0.0008	92.5	5.765	8.156	0.011	7.5
HT	Before exsolution	3.914	0.0009	63.5	5.67	8.026	0.0036	36.5
	After exsolution	3.907	0.00001	84.1	5.788	7.883	0.01	15.9
CP	Before exsolution	4.963	0.0061	7.3	5.521	7.85	0.0008	92.7
	After exsolution	3.911	0.001	89.9	5.769	7.963	0.015	10.1

Table S2. LSTN elements ratios (in precentage) as measured by XPS before and after sputtering and by EDX elemental analysis. Nominal ratios are calculated according to intended stoichiometry $Sr_{0.7}La_{0.2}Ti_{0.95}Ni_{0.05}O_{3-\delta}$.

		Sr	La	Ti	Ni	Sr/La	Ti/Ni
	nominal	36.8	10.5	50.0	2.6	3.5	19.0
SS	XPS before sputtering	42.4	10.3	46.8	0.5	4.1	93.6
	XPS after sputtering	42.2	14.0	43.3	0.5	3.0	86.6
	EDX	33.6	10.6	53.2	2.6	3.2	20.5
SG	XPS before sputtering	49.5	9.6	40.4	0.5	5.2	80.8
	XPS after sputtering	45.1	13.8	40.6	0.4	3.3	101.5
	EDX	32.5	9.3	53.5	4.7	3.5	11.4
HT	XPS before sputtering	36.4	25.9	34.6	3.1	1.4	11.2
	XPS after sputtering	42.8	20.4	36.0	0.9	2.1	40.0
	EDX	40.1	12.3	44.4	3.2	3.3	13.9
CP	XPS before sputtering	38.9	15.3	45.1	0.7	2.5	64.4
	XPS after sputtering	41.1	16.1	42.2	0.6	2.6	70.3
	EDX	31.9	11.1	54.6	2.3	2.9	23.7

Table S3. XPS binding energies (in eV) of LSTN elements signals before and after 3 minutes Ar sputtering. Full widths at half maximum (FWHM) are given in brackets. Secondary peaks are given below the main peaks.

		O 1s	Sr $3d_{5/2}$	ΔSr 3d	Ti $2p_{3/2}$	ΔTi 2p	La $3d_{5/2}$	ΔLa 3d	ΔLa 3d sat	La $4d_{5/2}$	ΔLa 4d	Ni $2p_{1/2}$	Ni 2p sat	Ni 3p
Before sputtering	SS		133.3 (1.1)	1.6	458.7 (1.1)	5.1	834.4 (3.1)	16.8	4.6	102.5 (2.6)	3.0			
			132.8 (2.5)		457.6 (2.1)		837.5 (2.1)	16.8						
	SG		132.8 (1.2)	1.6	458.2 (1.2)	5.5	833.9 (2.3)	16.7	4.5	101.9 (2.1)	3.1			
			132.0 (2)		457.5 (2)		836.4 (2.3)	16.8						
	HT		132.9 (1.2)	1.6	458.2 (1.3)	5.6	834.5 (2.6)	16.8	4.1	102.5 (2.4)	3.1	872.5 (2.4)	6.3	
			132.2 (1.9)		457.8 (2.1)		836.8 (1.9)	17.3				874.3 (2.4)		
	CP		132.9 (1)	1.7	458.3 (1.1)	5.8	834.1 (1.6)	16.9	4.5	102.2 (1.8)	3.1	872.7 (1.6)		
							835.7 (3.4)	16.6				874.2 (3)		
After sputtering	SS	529.9 (1.3)	133.2 (1.3)	1.7	458.3 (1.2)	5.3				102.2 (1.8)	3.1			65.8 (2.4)
		531.3 (2)			457.4 (4.5)									67.7 (2.3)
	SG	529.9 (1.4)	133.1 (1.4)	1.7	458.1 (1.3)	5.5				102.2 (1.8)	3.1			65.6 (2.2)
		531.6 (1.9)			457.0 (3.6)									67.6 (1.9)
	HT	530.0 (2)	133.4 (1.9)	1.8	458.3 (1.5)	5.4				102.0 (2.2)	3.1			66.1 (2.8)
		532.0 (1.6)			457.5 (2.3)									68.0 (2.5)
	CP	530.1 (1.3)	133.4 (1.3)	1.7	458.3 (1.2)	5.6				102.2 (1.8)	3.0			66.0 (2.4)
		531.7 (2)			457.0 (4)									67.9 (2.2)

Table S4. Resistivity values obtained from fitting the impedance spectra of fuel cells with LSTN-GDC anodes to the equivalent circuit shown in figure 6. R_s is the ohmic resistance, R_1 is from hiqh frequency impedance, R_2 is from medium frequency impedance, R_3 is from low frequency impedance, R_p is the total polarization resistivity equal to $R_1+R_2+R_3$ and σ is the conductivity according to the ohmic resistance and cell thickness.

		R_s (Ω cm^2)	R_1 (Ω cm^2) ~3 kHz	R_2 (Ω cm^2) ~6 Hz	R_3 (Ω cm^2) ~0.2 Hz	R_p (Ω cm^2)	σ (S/cm)
SS	Before stability	1.97	-	0.32	0.58	0.90	0.0054
	After stability	1.45	0.23	0.24	0.76	1.23	0.0074
SG	Before stability	1.98	-	0.38	0.60	0.99	0.0061
	After stability	1.75	-	0.48	0.70	1.18	0.0069
HT	Before stability	3.20	0.73	3.61	17.87	22.21	0.0032
	After stability	2.34	1.69	2.98	-	4.67	0.0044
CP	Before stability	1.81	-	0.54	0.96	1.49	0.0057
	After stability	1.35	0.20	0.75	0.36	1.31	0.0077

Supplementary Figures

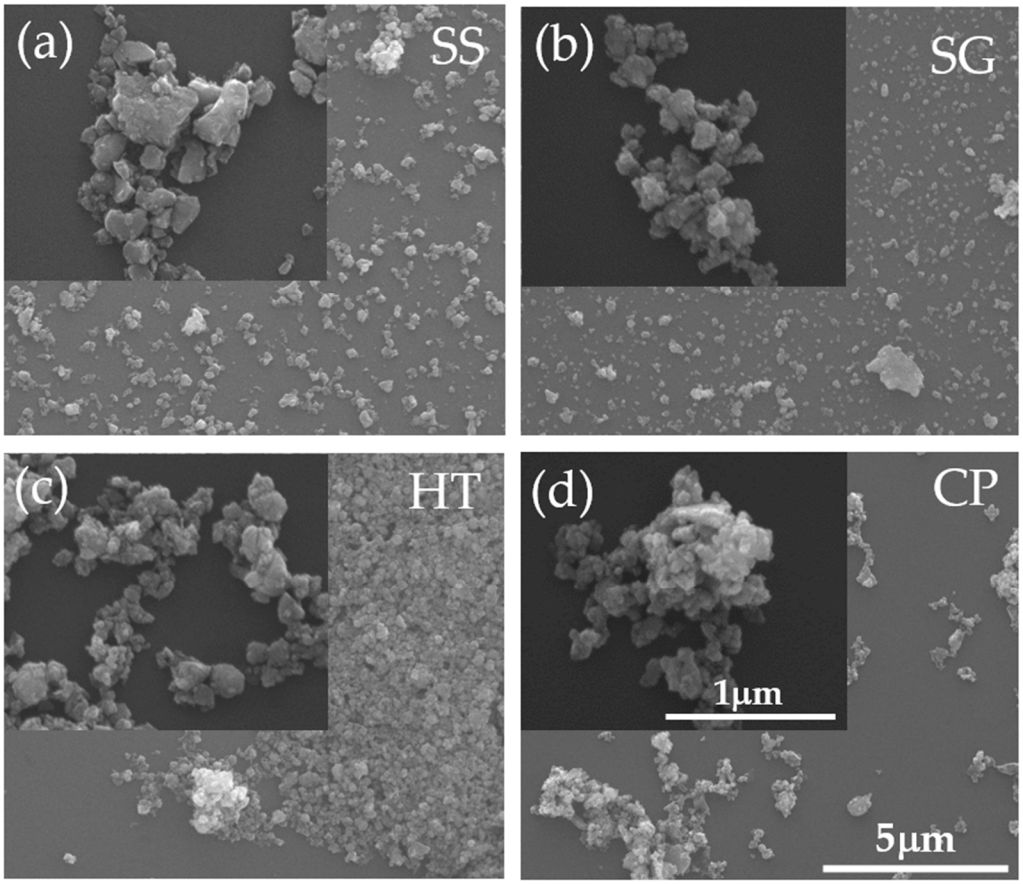

Figure S1. SEM micrographs of LSTN powders prepared by (a) solid state reaction (SS), (b) sol-gel (SG), (c) hydrothermal (HT) and (d) co-precipitation (CP) methods after identical ball milling process. Scale bars for CP sample apply for all.

(a)

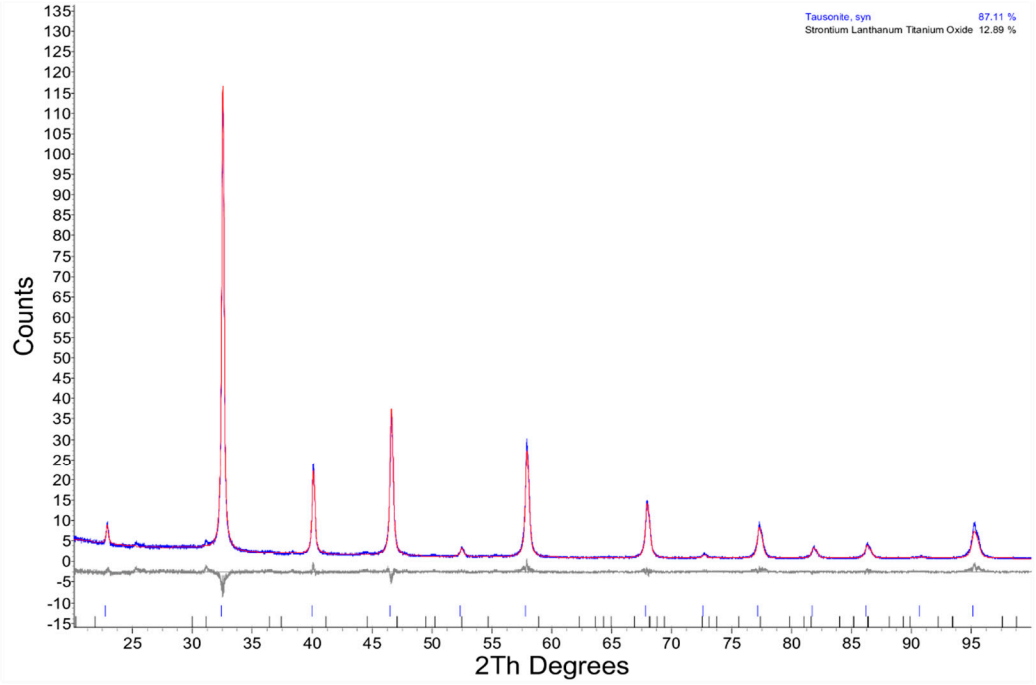
Tausonite, syn 87.11 %
Strontium Lanthanum Titanium Oxide 12.89 %
Counts
2Th Degrees

(b)

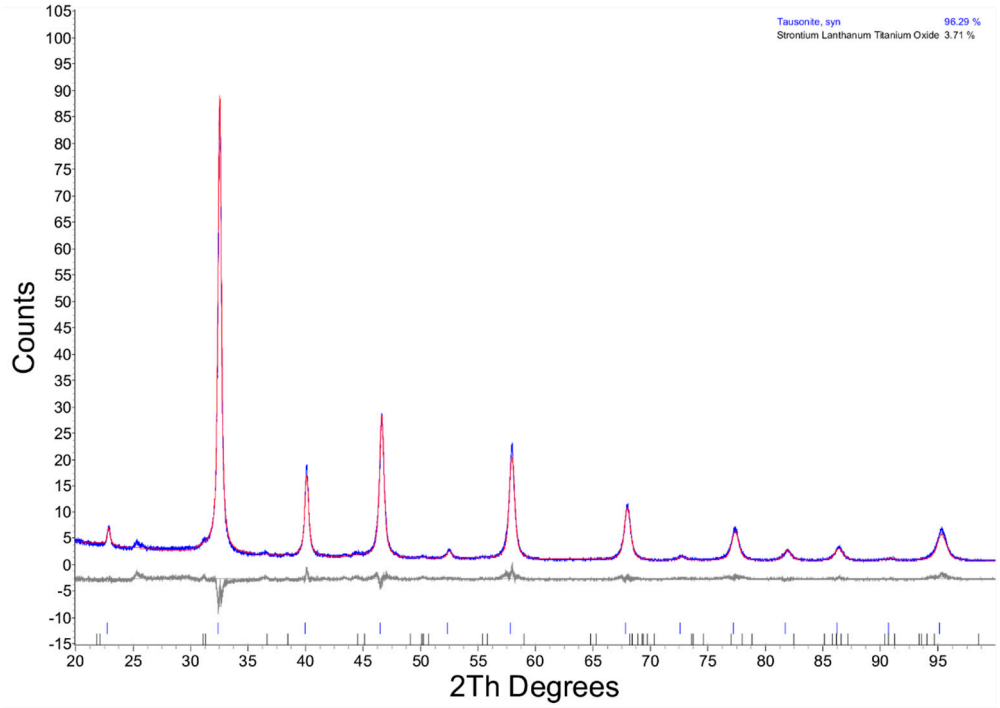
Tausonite, syn 96.29 %
Strontium Lanthanum Titanium Oxide 3.71 %
Counts
2Th Degrees

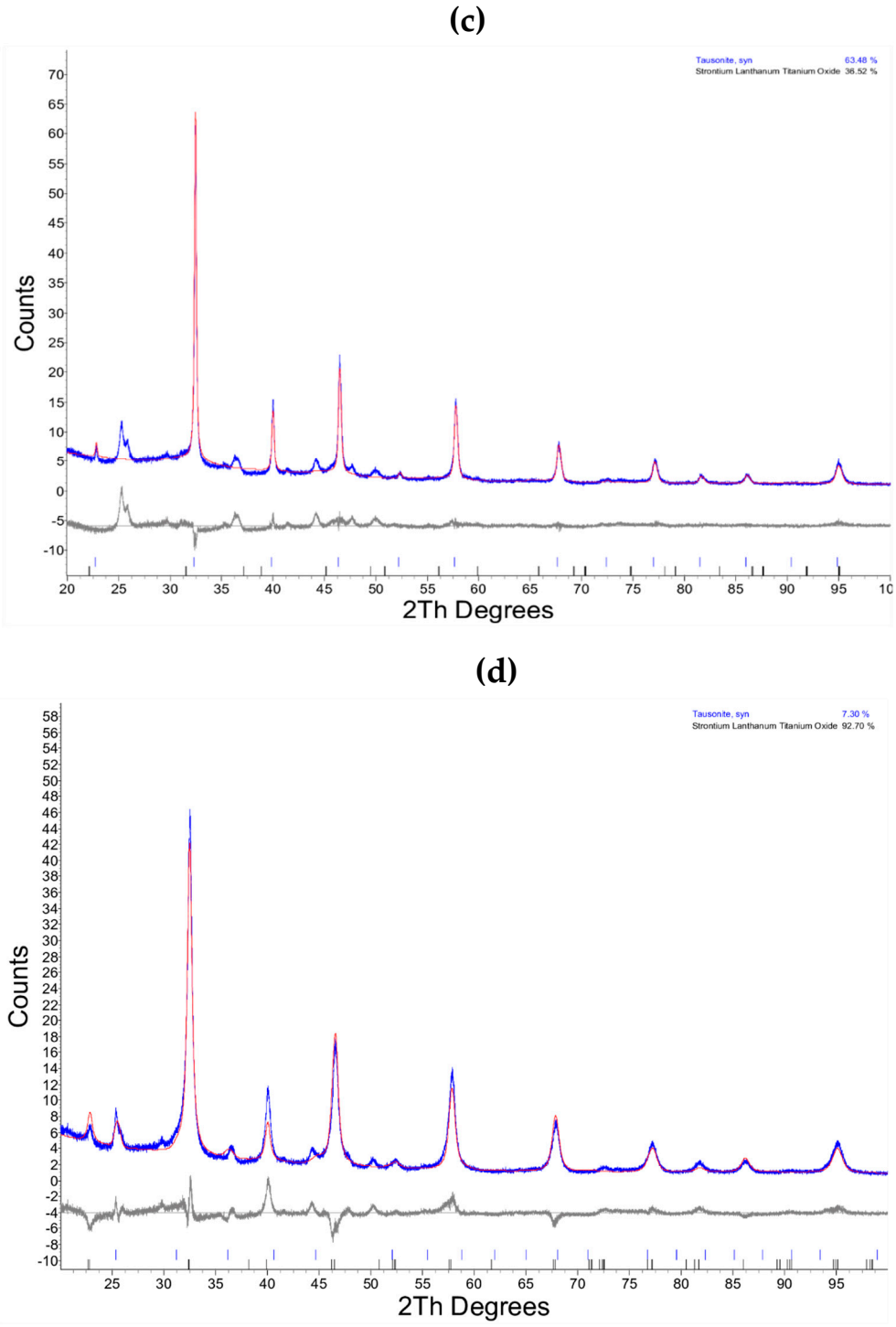

Figure S2. Rietveld refinement analysis of (a) solid state , (b) sol-gel, (c) hydrothermal and (d) coprecipitation LSTN samples before exsolution. The red lines indicate experimental data, the blue lines indicate simulated data, the lower grey traces indicate the difference between experimental and simulated data, and the blue and black vertical lines at the bottom indicate bragg's positions of cubic Pm-3m structure (PDF card no. 00-005-0634) and tetragonal I4/mcm (PDF card no. 04-025-4518), respectively.

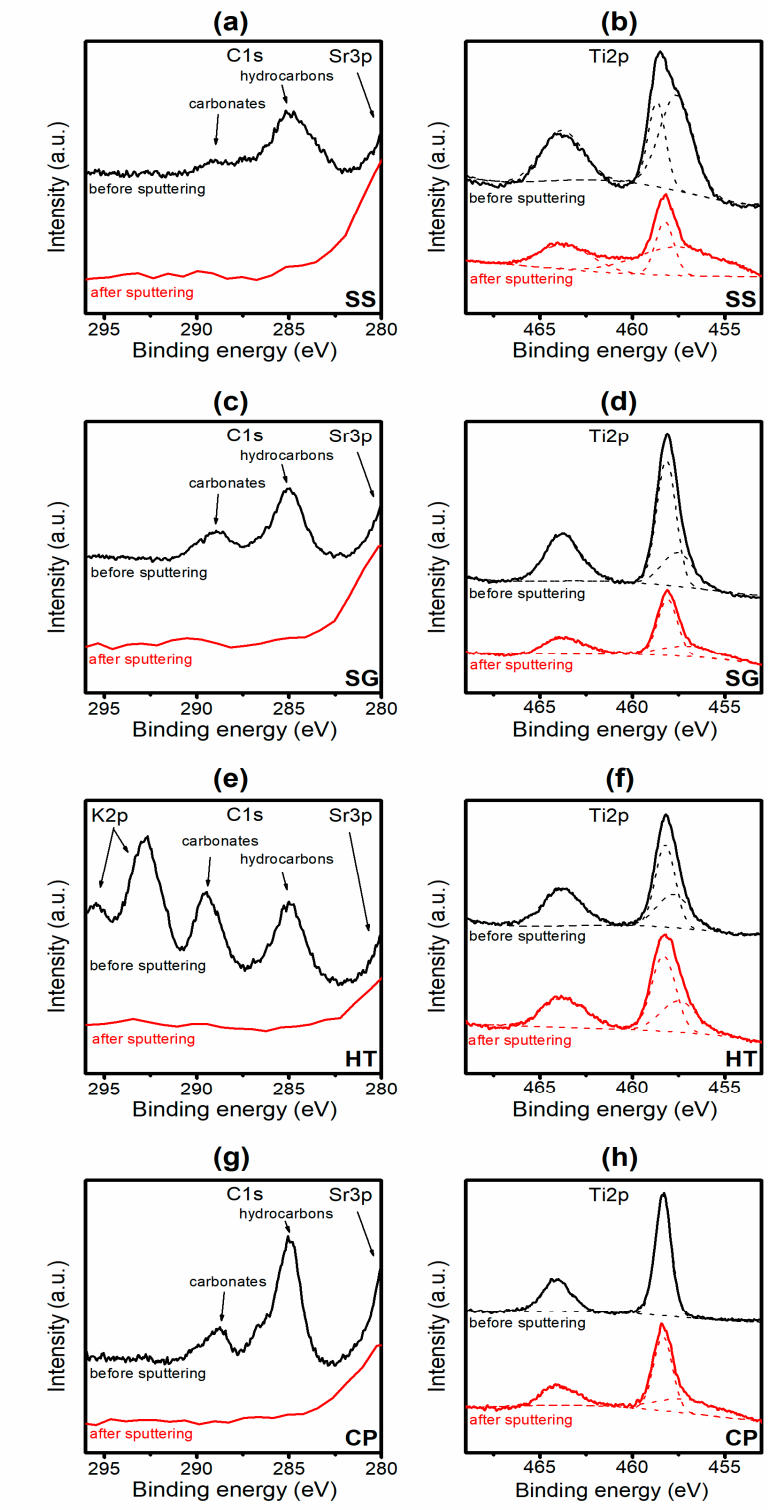

Figure S3. XPS spectra of C 1s and T 2p signals for LSTN powders before and after sputtering. (a) C 1s and (b) Ti 2p in solid state LSTN, (c) C 1s and (d) Ti 2p in sol-gel LSTN, (e) C 1s and (f) Ti 2p in hydrothermal LSTN, (g) C 1s and (h) Ti 2p in co-precipitation LSTN.

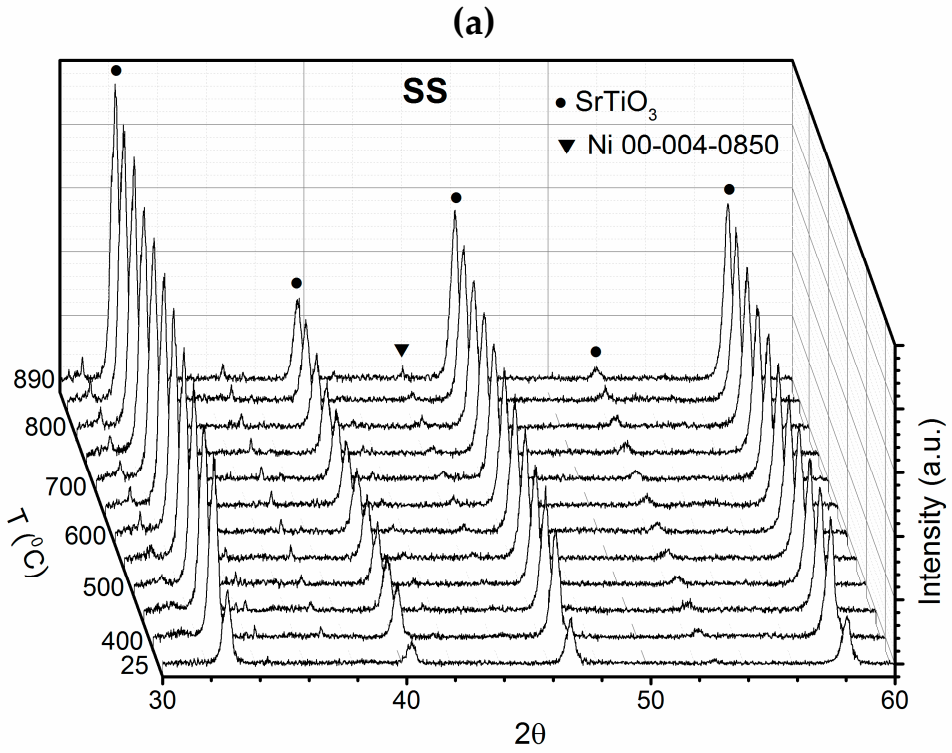
(a)
SS
• SrTiO3
▼ Ni 00-004-0850
890
800
700
600
500
400
25
T (°C)
30
40
50
60
2θ
Intensity (a.u.)

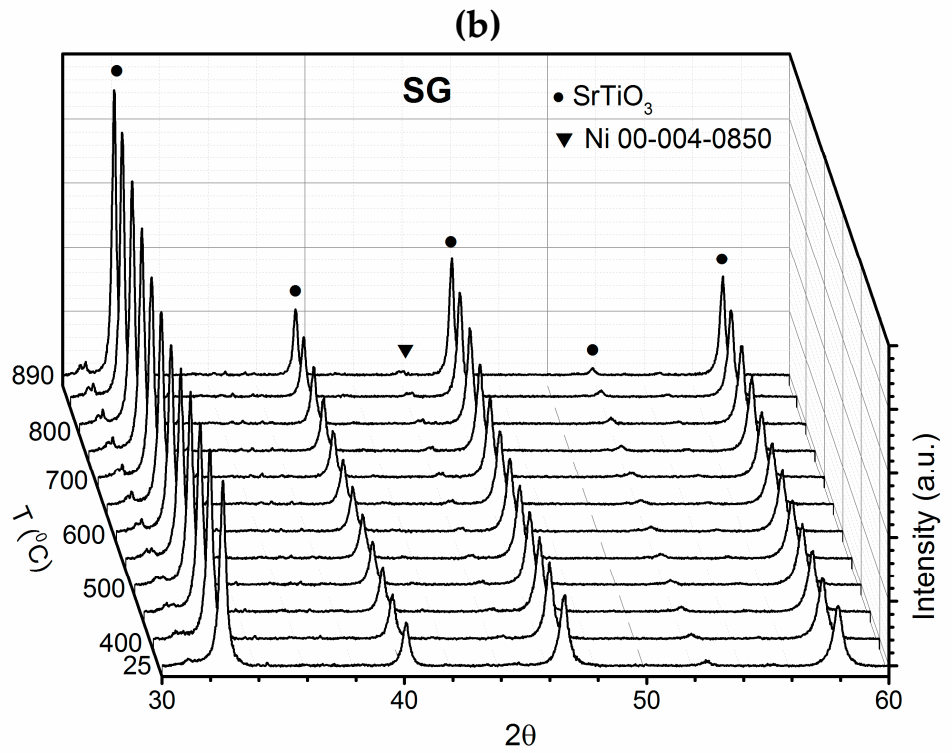
(b)
SG
• SrTiO3
▼ Ni 00-004-0850
890
800
700
600
500
400
25
T (°C)
30
40
50
60
2θ
Intensity (a.u.)

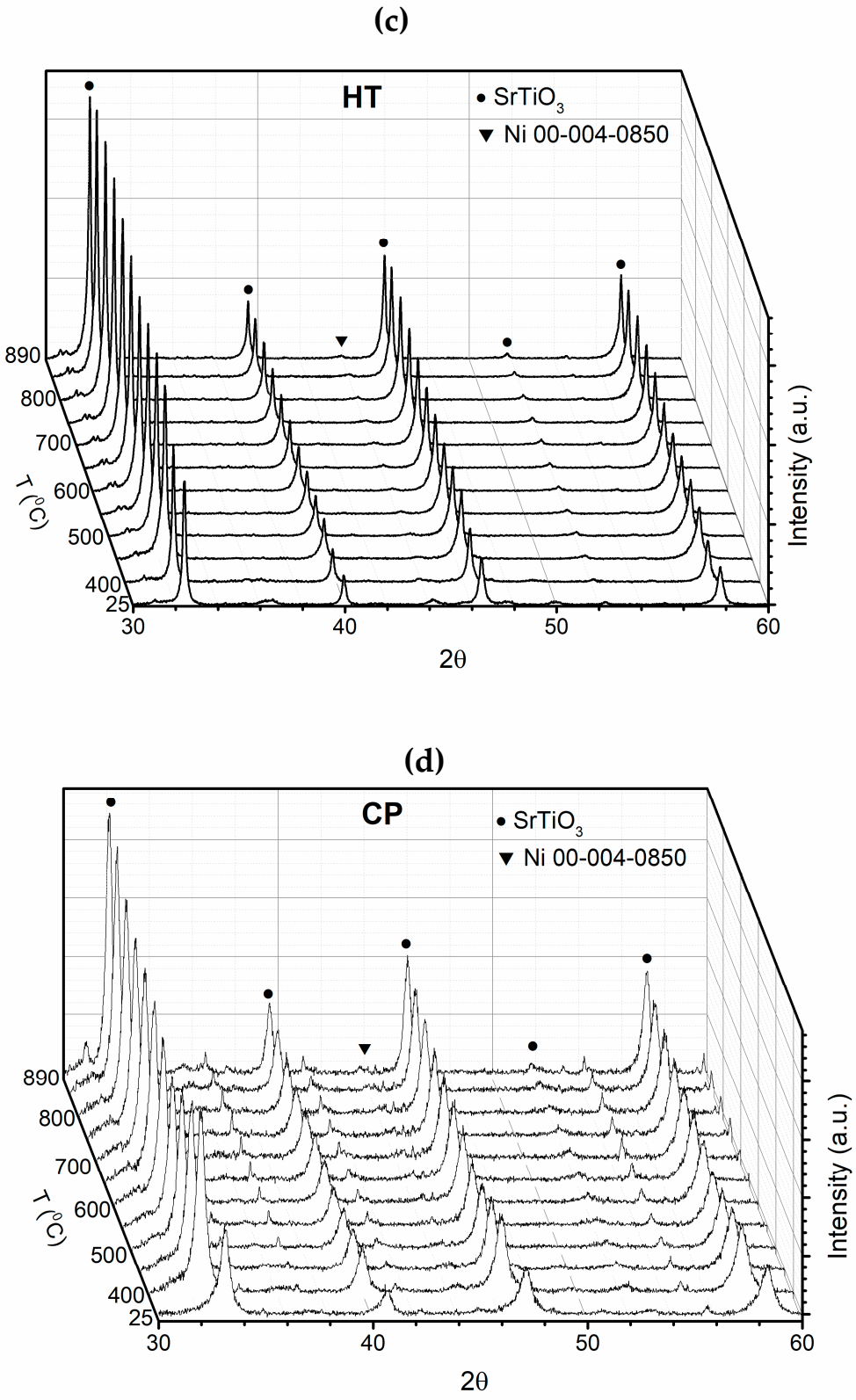

Figure S4. in situ XRD analysis of (a) solid state, (b) sol-gel, (c) hydrothermal, (d) coprecipitation LSTN powders under 5% H_2 in N_2 flow at R.T and between 400-890°C.

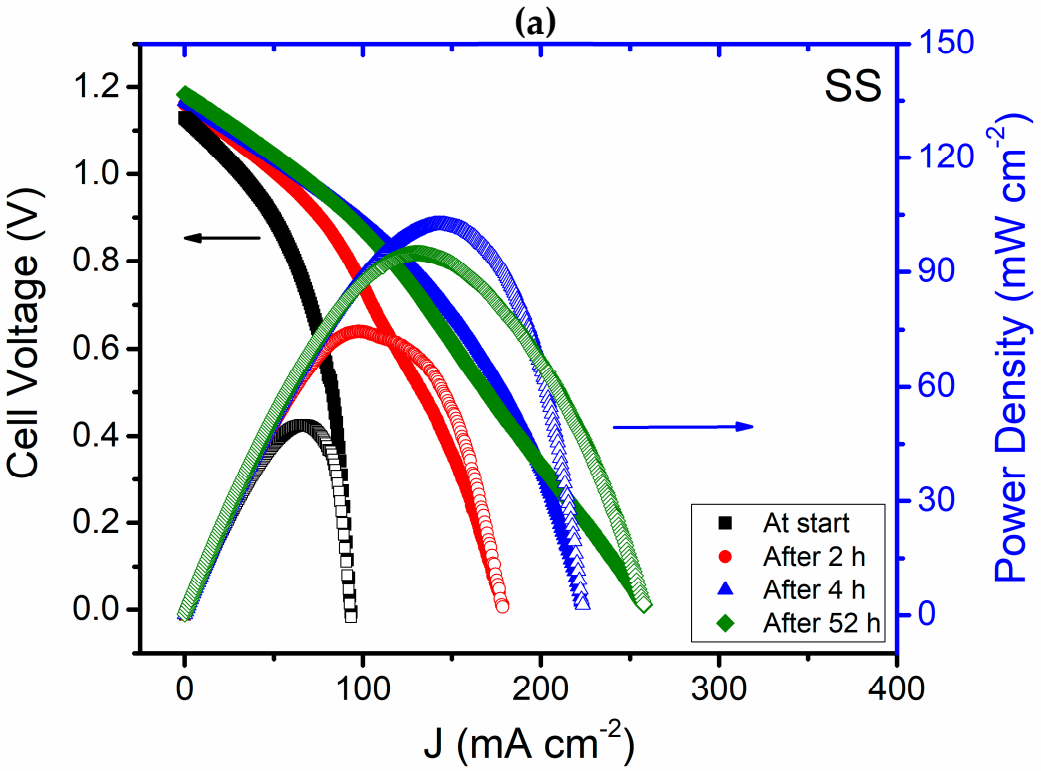
(a)
SS
Cell Voltage (V)
Power Density (mW cm-2)
J (mA cm-2)
At start
After 2 h
After 4 h
After 52 h

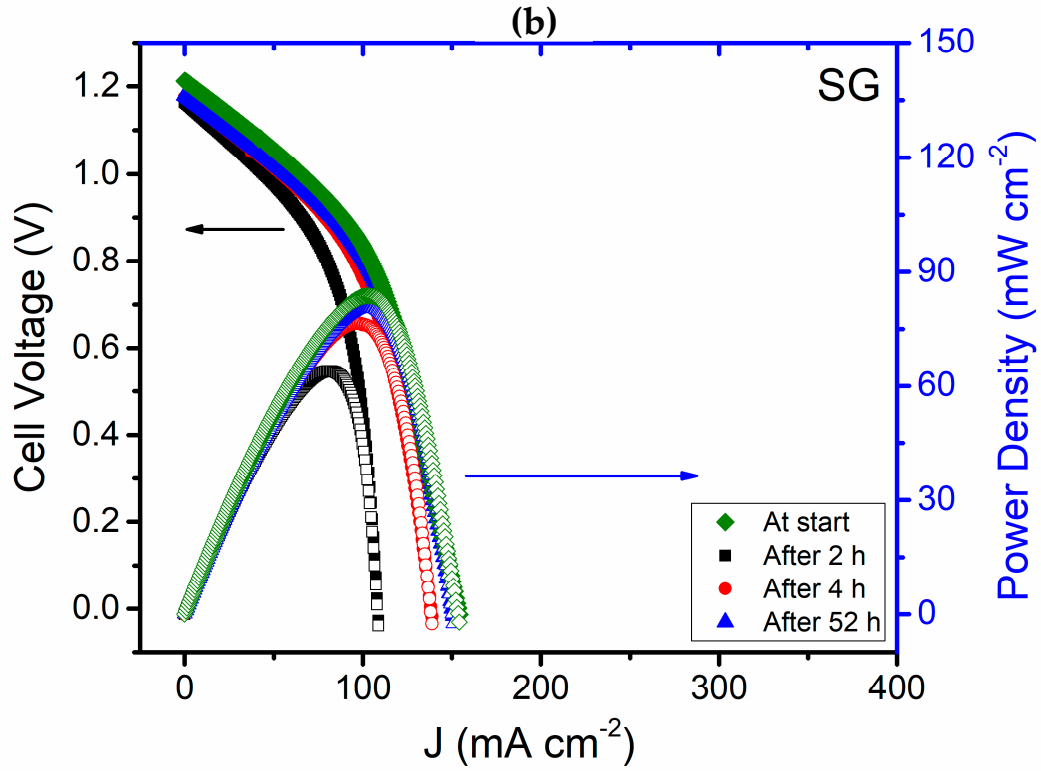
(b)
SG
Cell Voltage (V)
Power Density (mW cm-2)
J (mA cm-2)
At start
After 2 h
After 4 h
After 52 h

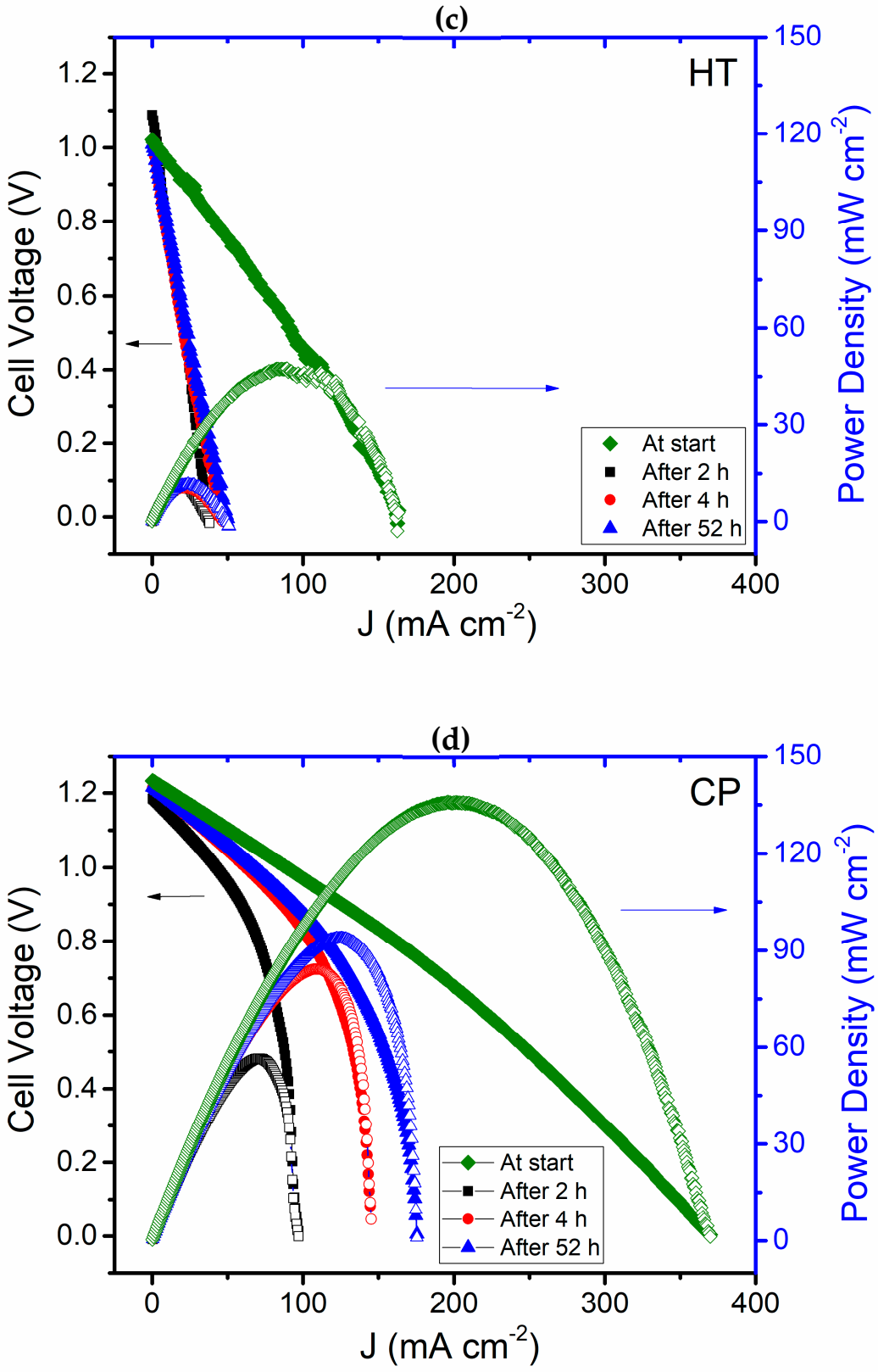

Figure S5. Polarization curves of fuel cells with of (a) solid state, (b) sol-gel, (c) hydrothermal, (d) coprecipitation LSTN-GDC anodes at different operation times at 820°C under 300 cm^3/min dry H_2 flow on anode side. The start time is defined when the cell reached the final operation temperature and hydrogen started to flow on the anode.

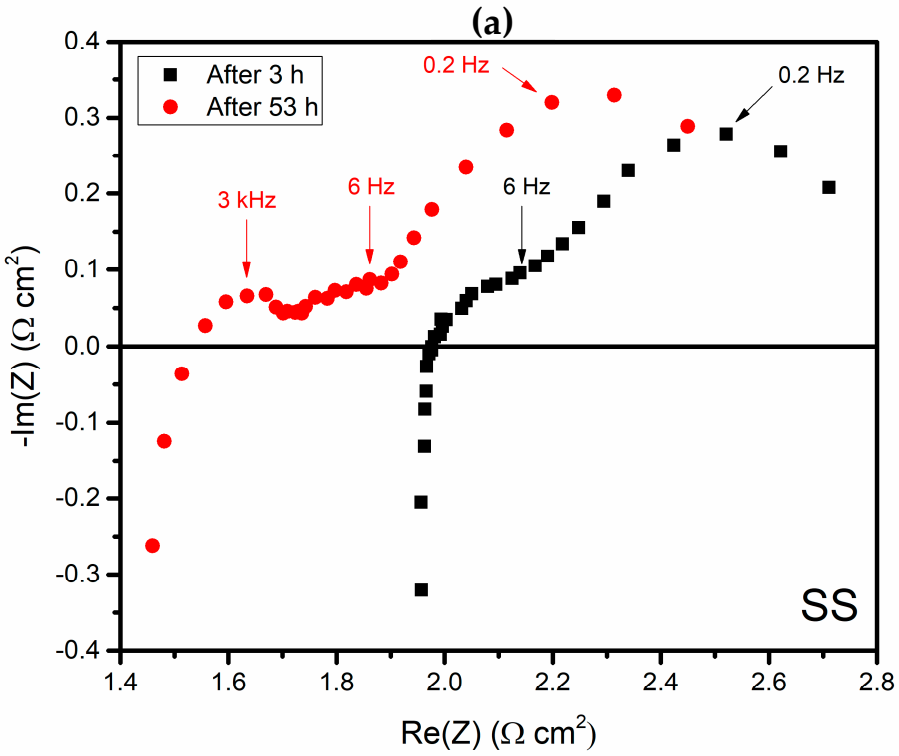
(a)
After 3 h
After 53 h
0.2 Hz
0.2 Hz
3 kHz
6 Hz
6 Hz
SS
-Im(Z) (Ω cm²)
Re(Z) (Ω cm²)

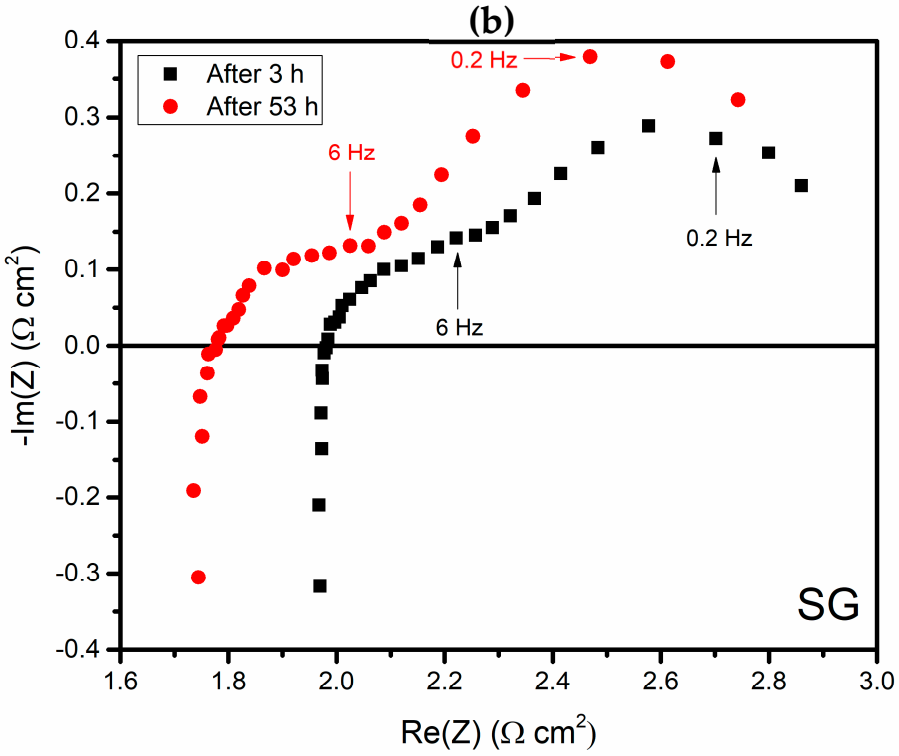
(b)
After 3 h
After 53 h
0.2 Hz
6 Hz
0.2 Hz
6 Hz
SG
-Im(Z) (Ω cm²)
Re(Z) (Ω cm²)

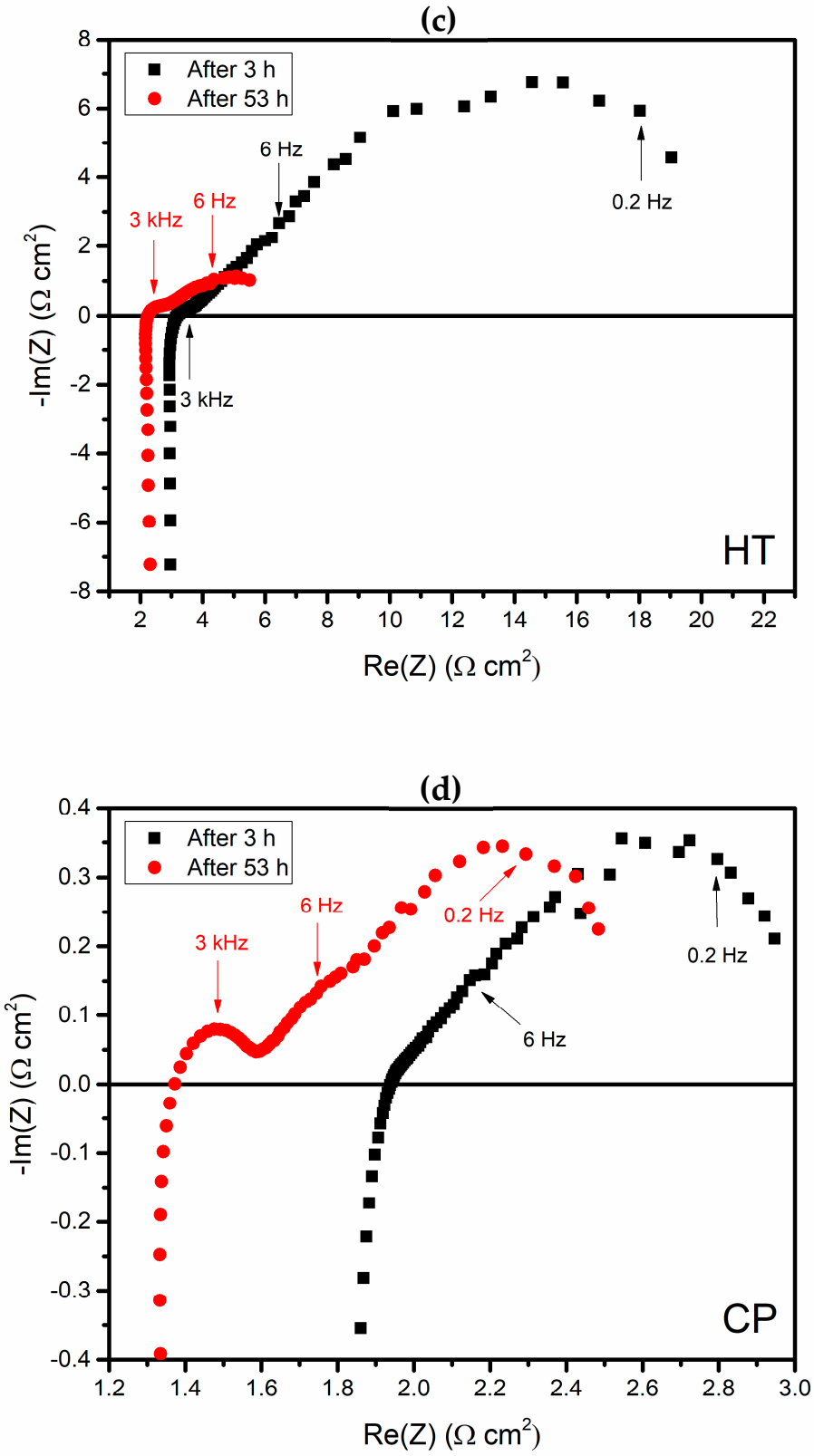

Figure S6. Impedance Nyquist plots of fuel cells with (a) solid state, (b) sol-gel, (c) hydrothermal, (d) coprecipitation LSTN-GDC anodes before and after 48 hours stability test. High frequency (HF, 3 kHz), medium frequency (MF, 6 Hz) and low frequency (LF, 0.2 Hz) are indicated.

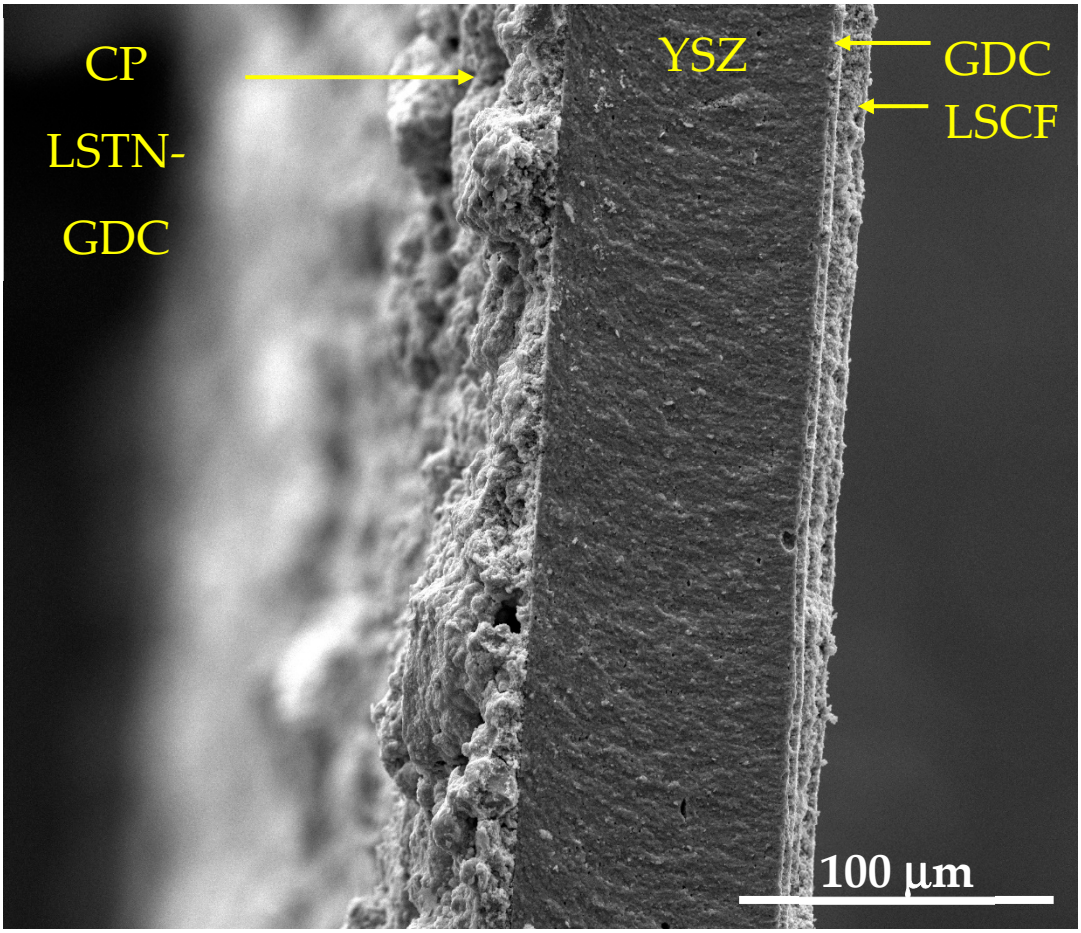

Figure S7. SEM micrograph of the cross-section of full fuel cell with CP LSTN-GDC anode after 48 hours stability testing.